BRIEF REPORTS

Brief Reports are short papers which report on completed research or are addenda to papers previously published in the **Physical Review.** *A Brief Report may be no longer than four printed pages and must be accompanied by an abstract.*

Target fragmentation of silver by 14.6 GeV/nucleon ^{16}O ions

M. Bronikowski and N. T. Porile
Department of Chemistry, Purdue University, West Lafayette, Indiana 47907
(Received 20 June 1991)

Cross sections for the production of target fragments in the interaction of silver with 14.6 GeV/nucleon ^{16}O ions have been measured and used to determine the mass-yield distribution. The results are compared with similar data obtained for other high-energy reactions and are generally consistent with factorization.

The availability in recent years of heavy-ion beams with energies >10 GeV/nucleon has made it of interest to extend target fragmentation studies to this new energy regime. In this Brief Report we present the mass-yield distribution of target fragmentation products of the interaction of silver with 14.6 GeV/nucleon ^{16}O ions. Similar studies have been previously performed in our laboratory with 2.1 GeV/nucleon ^{12}C ions [1] and with 300 GeV protons [1,2], which have nearly comparable total kinetic energy as the ^{16}O ions of present interest. Comparison with these previous studies permits a test of the limiting fragmentation and factorization hypotheses [3], which have been widely used to interpret target fragmentation induced by relativistic heavy ions. Previous studies with 13–15 GeV/nucleon heavy ions have shown deviations from limiting fragmentation in the recoil properties of light fragments formed from a range of targets [4]. However, consistency with this hypothesis was demonstrated for the mass-yield distribution of target fragmentation products from gold [5].

The experiments were performed at the Brookhaven Alternating Gradient Synchrotron (AGS). Targets consisted of 99.999% pure silver foils having a surface density of either 30 or 90 mg/cm^2, surrounded by two pairs of 100-μm-thick Mylar catcher foils and preceded by three 25-μm Al monitor foils. Six different irradiations were performed. Three of these had a duration of less than one hour and the other three lasted for 1–2 days. Total particle fluences ranged from 4×10^{10} to 9×10^{12}, as determined with a calibrated ionization chamber. Since this chamber was not available for all the irradiations, it was used to provide an internal monitor via the $^{27}Al(^{16}O,X)^{24}Na$ reaction, whose cross section was determined as 26±6 mb.

Following irradiation, the various foils were assayed with intrinsic Ge or Ge(Li) γ-ray spectrometers. Samples from the short irradiations were assayed at Brookhaven while those from the long irradiations were assayed at Purdue beginning approximately one day following the end of bombardment. The cross sections of some 90 nuclides were determined using techniques described in detail in previous reports from our laboratory [1,6,7]. The results are summarized in Table I, where the uncertainties are the larger of the standard deviation in the mean of replicate determinations and the estimated uncertainty in single determinations, as based on decay curve analysis. An additional 10% error was folded into the estimated uncertainty for nuclides whose cross sections were measured only once. Owing to uncertainties in beam monitoring, the systematic error in the cross sections is $\sim$25%. The results were corrected for variations in beam intensity during a given irradiation, where appropriate. We did not apply corrections for production by secondary particles, as it was shown previously [1] that such corrections are $<5\%$ for target thicknesses of present interest.

The tabulated data represent only a fraction of the total isobaric yields. The unmeasured cross sections were estimated by means of a modified form of the Rudstam equation [8], as described in detail elsewhere [1]. The measured cross sections were fitted with the following 10-parameter equation:

$$\sigma(Z,A)=\exp[\alpha_1+\alpha_2 A+\alpha_3 A^2+\alpha_4 A^3 +(\alpha_5+\alpha_6 A+\alpha_7 A^2)|Z_p-Z|^{\alpha_8}] , \qquad (1)$$

where the most probable charge Z_p is parametrized as

$$Z_p=\alpha_9 A+\alpha_{10} A^2 . \qquad (2)$$

The parameters α_1–α_4 determine the shape of the mass-yield distribution while α_5–α_{10} determine the isobaric yield distribution at each mass number. An iterative nonlinear least-squares code [9] was used to fit the data. In the first iteration, both cumulative and independent yields were fitted. Next, the calculated progenitor cross sections were subtracted from the cumulative yields and the resulting independent yields were refitted. The iterations were repeated three additional times by which point the cross sections converged to virtually constant values.

The parameters $\alpha_1-\alpha_{10}$ are summarized in Table II. Figure 1 shows a comparison of the fractional isobaric yield distribution at $A=70$ with the data, scaled to this mass number by the ratio of calculated cross sections at $A=70$ and the mass number in question [1]. The parametrization adequately fits the data. The cross sections of measured nuclides were estimated by means of Eq. (1). The experimental mass-yield distribution was obtained by adding the estimated cross sections to the experimental values at a given mass number. In arriving at the indicat-

TABLE I. Cross sections (mb) for the formation of target fragmentation products in the reaction of Ag with 14.6 GeV/nucleon ^{16}O.

^{22}Na	C+ [a]	9.34±0.64	^{86}Y^m	I	16.0±0.3
^{24}Na	C− [b]	19.0±0.3	^{86}Zr	C+	11.6±0.1
^{28}Mg	C−	2.46±0.08	^{87}Y^m	C+	41.9±0.9
^{39}Cl	C−	1.66±0.17	^{88}Y	I	6.06±0.03
^{43}K	C−	2.81±0.08	^{88}Zr	C+	36.4±0.5
^{43}Sc	C+	2.41±0.51	^{89}Zr	C+	38.4±1.2
^{44}Sc^g	I [c]	3.16±0.67	^{89}Nb [f]	PC+	2.32±0.38
^{44}Sc^m	I	5.65±0.21	^{90}Nb^g	I	18.6±1.1
^{46}Sc	I	8.72±0.34	^{90}Mo	C+	8.26±0.17
^{47}Ca	C−	0.246±0.023	^{92}Nb^m	I	1.20±0.08
^{48}Sc	I	1.07±0.01	^{93}Mo^m	I	7.11±0.21
^{48}V	C+	7.00±0.23	^{93}Tc^g	PC+	9.05±3.14
^{52}Mn^g	I	4.37±0.14	^{94}Tc^g	I	15.5±0.7
^{54}Mn	I	16.4±1.3	^{94}Tc^m	C+	4.69±0.44
^{56}Co	C+	3.04±0.23	^{94}Ru	C+	4.79±0.17
^{57}Co	C+	8.98±0.23	^{95}Nb^m	I	1.75±0.22
^{58}Co	I	15.3±1.3	^{95}Tc^g	PC+	34.5±1.2
^{59}Fe	C−	1.60±0.04	^{95}Tc^m	PC+	2.66±0.07
^{65}Zn	C+	18.6±1.0	^{95}Ru	C+	14.9±0.5
^{67}Ga	C+	20.9±1.4	^{96}Nb	I	0.431±0.074
^{67}Ge	C+	2.12±0.08	^{96}Tc	I	15.1±0.8
^{69}Ge	C+	13.3±0.8	^{97}Ru	C+	43.4±1.3
^{71}As	C+	15.2±0.6	^{97}Rh^g	PC+	6.65±0.27
^{72}As	I	14.0±1.0	^{98}Rh	I	17.1±2.4
^{72}Se	C+	3.88±0.10	^{98}Pd	C+	0.853±0.131
^{73}Se	PC+ [d]	9.09±0.12	^{99}Mo	C−	0.414±0.022
^{74}As	I	4.34±0.05	^{99}Rh^g	I	5.71±0.01
^{75}Se	C+	21.8±0.5	^{99}Rh^m	I	27.8±0.7
^{75}Br	C+	8.96±0.25	^{99}Pd	C+	4.17±0.14
^{76}Br	I	11.1±0.7	^{100}Rh	I	22.4±2.8
^{76}Kr	C+	4.59±0.27	^{100}Pd	C+	14.2±0.7
^{77}Br	C+	20.8±0.3	^{101}Rh^g	I	14.1±1.4
^{77}Kr	C+	8.70±0.32	^{101}Rh^m	I	29.2±1.7
^{79}Kr	C+	23.1±0.2	^{101}Pd	C+	27.5±0.9
^{81}Rb^g	PC+	33.7±1.5	^{102}Rh^g	I	12.4±1.1
^{81}Sr	C+	4.88±0.32	^{102}Rh^m	I	7.67±0.18
^{82}Rb^m	I	9.01±0.90	^{103}Ru	C−	2.34±0.08
^{83}Rb	C+	32.5±1.1	^{103}Ag	C+	15.7±1.2
^{83}Sr	C+	24.2±1.3	^{104}Ag^g	PC+	19.5±0.8
^{84}Rb	I	3.57±0.21	^{104}Ag^m	C+	20.4±0.8
^{84}Y [e]	C+	6.77±0.25	^{105}Rh	C−	10.9±0.6
^{85}Sr^g	PC+	42.8±1.0	^{105}Ag	C+	77.4±4.6
^{85}Y^g	PC+	1.99±0.19	^{106}Rh^m	I	3.39±0.87
^{85}Y^m	PC+	22.4±1.1	^{106}Ag^m	I	22.8±1.7
^{86}Rb	I	0.905±0.166	^{110}Ag^m	I	51.8±1.1

[a] C+, cumulative yield; includes cross sections of more neutron-poor isobaric progenitors.

[b] C−, cumulative yield; includes cross sections of more neutron-rich isobaric progenitors.

[c] I, independent yield.

[d] PC+, partial cumulative yield.

[e] 40 min isomer.

[f] 66 min isomer.

TABLE II. Parameters from the fit of Eq. (1) to the target fragmentation cross sections for Ag+14.6 GeV/nucleon ^{16}O.

α_1	4.16 ± 0.11	α_6	$(-3.28\pm0.26)\times10^{-2}$
α_2	$(-6.94\pm0.62)\times10^{-2}$	α_7	$(3.00\pm0.18)\times10^{-4}$
α_3	$(8.90\pm1.02)\times10^{-4}$	α_8	1.56 ± 0.02
α_4	$(-2.62\pm0.52)\times10^{-6}$	α_9	0.482 ± 0.003
α_5	-0.600 ± 0.092	α_{10}	$(-3.22\pm0.04)\times10^{-4}$

ed uncertainties in the isobaric yields the estimated cross sections were assigned 25% errors, based on the agreement between measured independent yields and Eq. (1). Figure 2 shows the resulting mass-yield distribution where the solid curve, obtained by summation of Eq. (1) over all contributing Z at a given A, provides a good fit to the data. The isobaric yields decrease continuously from the target to a broad minimum at $A\sim50$ and increase slightly for $A\lesssim30$. This behavior is similar to that observed for 2 GeV/nucleon ^{12}C ions and presumably reflects a similar combination of spallation, fission, and fragmentation mechanisms as at lower energy.

Sümmerer *et al.* [10] have recently proposed a new empirical parametrization of spallation cross sections and have derived numerical values for their parameters by fitting literature data for high-energy reactions of targets with $A\gtrsim50$. The dashed curves in Figs. 1 and 2 show fits to our data obtained with this parametrization. The isobaric yield distribution is shifted slightly towards more neutron-rich products than Eq. (1), but fits the data equally well. The mass-yield distribution is assumed to be exponential and fits the data over a limited mass range. It obviously cannot fit the data for $A\lesssim60$, where

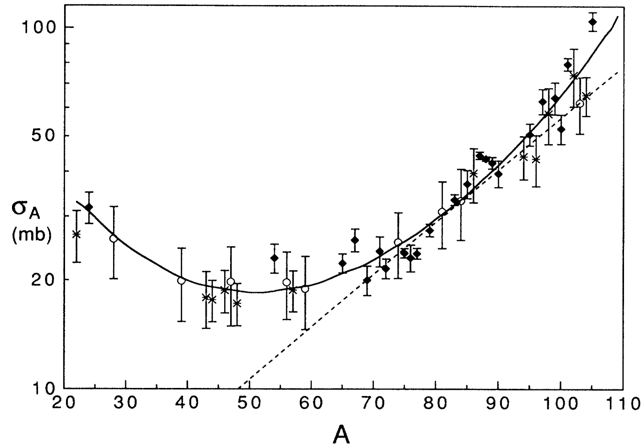

FIG. 2. Mass-yield distribution for the interaction of Ag with 14.6 GeV/nucleon ^{16}O ions. The various symbols indicate the fraction of the total isobaric yield at each mass number represented by the data in Table I: ♦, >50%, ∗, 20–50%; ○, <20%. Solid curve, from Eq. (1); dashed curve, from Sümmerer parametrization [10].

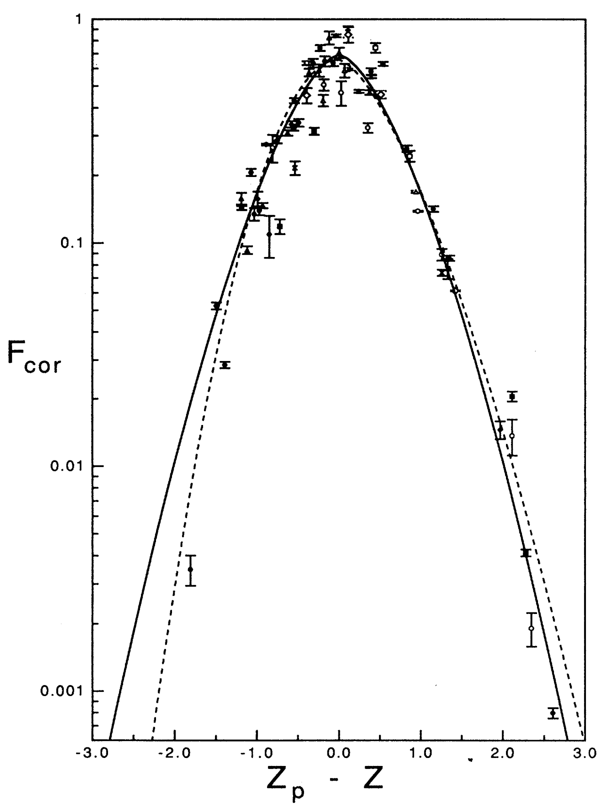

FIG. 1. Fractional isobaric yield distribution at $A=70$. Solid curve, from Eq. (1); dashed curve, from Sümmerer parametrization [10]. The experimental points for nuclides in different mass regions (⧗, $A=21$–40; ♦, 41–60; ▲, 61–80; ●, 81–100; ■, >100) have been scaled to $A=70$. Open points, independent yields; closed points, corrected cumulative yields.

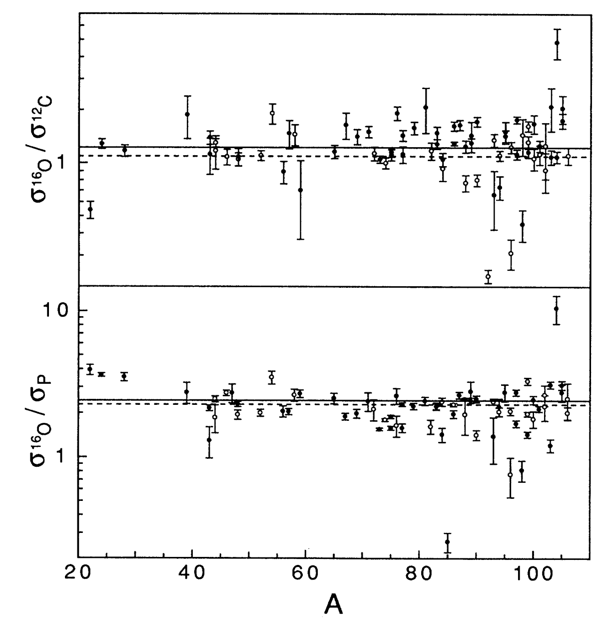

FIG. 3. Mass dependence of cross section ratios: top, $\sigma_{14.6\ \mathrm{GeV/nucleon}\ ^{16}\mathrm{O}}/\sigma_{2.1\ \mathrm{GeV/nucleon}\ ^{12}\mathrm{C}}$; bottom, $\sigma_{14.6\ \mathrm{GeV/nucleon}\ ^{16}\mathrm{O}}/\sigma_{300\ \mathrm{GeV\ p}}$. Solid line, ratio of experimental σ_R; dashed line, ratio of calculated σ_R. Closed points, cumulative yields; open points, independent yields.

TABLE III. Isomer ratios σ_m/σ_g of independently formed products in reactions of Ag with high-energy P, ^{12}C, and ^{16}O.

Nuclide	$I\pi(m)^{a}$ / $I\pi(g)$	P	^{12}C	^{16}O
^{44}Sc	$6+/2+$	1.33±0.06	1.61±0.06	1.79±0.21
^{99}Rh	$\frac{9}{2}+/\frac{1}{2}-$	2.89±0.07	3.96±0.10	4.87±0.02
^{102}Rh	$2-/6+$	0.51±0.24[b]	0.86±0.42[b]	0.62±0.09

[a] Spin-parity of metastable state/spin-parity of ground state.
[b] The data for the two isomers in Ref. 1 are reversed.

the experimental mass-yield distribution begins to flatten out.

Figure 3 shows a comparison of the experimental cross sections with the corresponding values for the interaction of Ag with 2.1 GeV/nucleon ^{12}C and with 300 GeV protons [1]. Factorization demands that the ^{16}O cross sections be larger than the ^{12}C or proton cross sections by the ratio of the respective total reaction cross sections, σ_R. The σ_R were evaluated with the soft spheres model [11]. Experimental σ_R values were obtained from the fits of Eq. (1) by integration of the mass yield distributions over A for $30 \leq A \leq 100$, the mass interval fitted in the ^{12}C and proton experiments.

The calculated σ_R ratios are some 10% smaller than the experimental ratios, which is well within the uncertainty in the absolute values of the cross sections. The individual cross-section ratios scatter about the mean values. Occasional large discrepancies may be noted. For example, the cross section for the formation of ^{104}Ag^m is much larger for ^{16}O than for either ^{12}C or protons, while that for ^{96}Nb is much lower. However, the only systematic difference may be noted for the ^{16}O$/p$ ratios for light fragments, which are nearly a factor of 2 larger than the σ_R ratios. This departure from factorization, which has been observed previously [1,5,6,12] has been attributed to the role of central collisions in light fragment production. We do not see any evidence of enhanced yield of the one- and two-neutron removal reactions induced by ^{16}O. Enhancements in these reaction channels due to electromagnetic dissociation have been reported previously [5,13,14] particularly for heavy element targets interacting with heavy projectiles. Unfortunately, silver is not a favorable target to observe this effect because of the presence of two stable isotopes and the occurrence of isomerism in the reaction products.

We have obtained isomer ratios for three independently formed products in the present work as well as in the previously reported [1] 2.1 GeV/nucleon ^{12}C and 300 GeV proton reactions. The results are summarized in Table III. The ratio of high-spin to low-spin state yields generally increases with projectile mass, and for the heavy ions, with energy. Evidently, at these high energies there are still significant differences in the angular momentum in the entrance channel, and they play a noticeable role in the deexcitation process.

This work was part of the E825 experiment at the Alternating Gradient Synchrotron (AGS). We wish to acknowledge the assistance and collaboration of the other members of this group: Y. Y. Chu, J. B. Cumming, P. E. Haustein, S. Katcoff, W. Loveland, K. Aleklett, and L. Sihver. This research was supported by the U.S. Department of Energy.

[1] N. T. Porile, G. D. Cole, and C. R. Rudy, Phys. Rev. C **19**, 2288 (1979).
[2] G. English, Y. W. Yu, and N. T. Porile, Phys. Rev. C **10**, 2268 (1974).
[3] A. S. Goldhaber and H. H. Heckman, Annu. Rev. Nucl. Part. Sci. **28**, 161 (1978).
[4] W. Loveland, K. Aleklett, M. Bronikowski, Y. Y. Chu, J. B. Cumming, P. E. Haustein, S. Katcoff, N. T. Porile, and L. Sihver, Phys. Rev. C **37**, 1311 (1988).
[5] W. Loveland, M. Hellström, L. Sihver, and K. Aleklett, Phys. Rev. C **42**, 1753 (1990).
[6] G. D. Cole and N. T. Porile, Phys. Rev. C **24**, 2038 (1981).
[7] D. L. Klingensmith and N. T. Porile, Phys. Rev. C **38**, 818 (1988).
[8] G. Rudstam, Z. Naturforsch. **21a**, 1027 (1966).
[9] J. B. Cumming, P. E. Haustein, R. W. Stoenner, L. Mausner, and R. A. Naumann, Phys. Rev. C **10**, 739 (1974).
[10] K. Sümmerer, W. Brüchle, D. J. Morrissey, M. Schädel, B. Szweryn, and Y. Weifan, Phys. Rev. C **42**, 2546 (1990).
[11] P. J. Karol, Phys. Rev. C **11**, 1203 (1975).
[12] S. B. Kaufman, E. P. Steinberg, B. D. Wilkins, and D. J. Henderson, Phys. Rev. C **22**, 1897 (1980).
[13] M. T. Mercier, J. C. Hill, F. K. Wohn, and A. R. Smith, Phys. Rev. Lett. **52**, 898 (1984).
[14] J. C. Hill, F. K. Wohn, J. A. Winger, M. Khayat, and M. T. Mercier, Phys. Rev. C **39**, 524 (1989).